Proceedings of the ASME 2011 International Mechanical Engineering Congress & Exposition
IMECE2011
November 11-17, 2011, Denver, Colorado, USA

IMECE2011-62648

THEORETICAL AND EXPERIMENTAL ANALYSES OF ENERGY EFFICIENT AIR DEHUMIDIFICATION SYSTEMS FOR TROPICAL CLIMATES USING MEMBRANE TECHNOLOGY

Zaw KHIN
Solar Energy Research Institute of Singapore (SERIS)
Singapore

Kim Choon NG
National University of Singapore (NUS)
Singapore

ABSTRACT

This paper presents the analytical and experimental analysis of a membrane based air-dehumidification system for handling the latent loads efficiently. This is important for tropical countries like Singapore where the humidity content of ambient air is high and therefore, air conditioning systems need to handle large latent load. A detailed COMSOL simulation model was set-up in order to simulate the water diffusion through the membrane. Experimental results from a real size membrane dehumidification unit are used to validate the mathematical model. Our investigations show that the moisture content of ambient air may be reduced by more than 5 g per kg of air if the dehumidification process is driven by the gradient between the water content of ambient air and the water content of exhaust air form air-conditioned spaces. With the exception of low electricity requirement for air transport, there is no electric energy consumption in the system. Therefore, the membrane system discussed in this paper is an efficient and alternative way of air dehumidification for air conditioning applications, potentially reducing the electricity consumption of air conditioning system in tropics.

Keywords: air dehumidification, membrane, energy saving, moisture transport, latent load, sensible load.

INTRODUCTION

A rising installation of air conditioning units leads to a growing energy demand in many regions of the world. In tropical climates, the latent loads constitute a large portion (approximately 75%) of the total cooling loads handled by an air conditioning unit due to the high humidity content in the ambient air (assuming ambient air of 32 ˚C and 70% relative humidity and supply air condition of 22 ˚C and 50% relative humidity). Thus, handling latent loads is critical to optimize air conditioning systems, particularly in tropical countries.

Many theoretical and experimental analyses [1-6] were carried out on thermally driven desiccant dehumidifiers – liquid desiccant [2] and solid desiccant dehumidifiers – for removing the moisture from the ambient air because of its energy saving and environmental friendliness. However, it is noted that a heat source is necessary for the regeneration of the desiccant materials, and thus, a solar thermal system or an industrial waste hear recovery system need to be installed.

Alternatively, the dehumidification can be performed by membrane technologies that demand almost no electric energy except for air transport. Research have been done [7-12] on the development and the investigation of the membrane technologies for different applications. Transfer of moisture and hydrochloric acid (HCL) through the membrane was studied by Tomaszewska et al. [7]. Moisture and heat transfer processes through the membrane-based heat exchanger or membrane dehumidification unit using different membrane materials [8] and different configuration of membrane heat exchangers [9, 10] have been investigated. Apart from using membrane layer only, Liu et al., [13] examined two coating methods applying on the membrane – solid desiccant ($CaCl_2$) coating and liquid desiccant (LiCl) coating on the fibre typed membrane. Therefore, the dehumidification capacity of the membrane unit increases due to the properties of solid and liquid desiccant materials. Additionally, a hygroscopic liquid membrane impregnated with a type of hygroscopic liquid was developed by Ito [14]. The hygroscopic liquid membrane comprised of two layers: the first layer being a hydrophilic membrane impregnated with a type of hygroscopic liquid, and the second layer being a hydrophobic membrane ensuring that the hygroscopic liquid did not enter into the second layer hydrophobic membrane. During the process of dehumidification, the process air was supplied along the surface of the hygroscopic liquid membrane while a high vacuum was applied on the other side of the liquid membrane. From the

studies, it is found that (i) the moisture transfer through membranes is highly influenced by both membrane properties and operating conditions, i.e., the gradient of moisture content in air streams; (ii) heat transfer also occurs due to the temperature difference between the two air streams; (iii) membrane technologies can be implemented for air dehumidification process with the merit of energy saving and environmental friendliness as it consumes no thermal energy and no electric energy, except for air transport.

In this paper, the investigation of air dehumidification using membrane technologies in the air conditioning applications is extended. Using the commercial finite element software COMSOL, a simplified three dimensional finite element model is constructed for a membrane air dehumidification unit. Subsequent experiment was carried out to verify the numerical results and to determine the mass transfer effectiveness. The results suggest to apply the membrane unit for air dehumidification in HVAC applications with significant energy saving.

NOMENCLATURE

D	Mass diffusion coefficient (m^2/s)
c	Moisture concentration (mol/m^3)
$\mathbf{u}$	Air velocity vector (m/s)
k	Convective mass transfer coefficient (m/s)
$\mathbf{n}$	Unit normal vector
L	Characteristic length (m)
Sh	Sherwood number (-)
Re	Reynold number (-)
Sc	Schmidt number (-)
ω	Humidity ratio (g/kg)

Subscripts

s	Supply air
e	Exhaust air
m	Membrane

MEMBRANE DEHUMIDIFICATION SYSTEM

A membrane-based air dehumidification system is simulated and experimentally tested for the Singapore Climate. A typical membrane based heat exchanger or membrane air dehumidification unit is shown in Fig. 1: two air streams – a wet air stream from the ambient (supply air) and a cold air stream from a conditioned room (exhaust air stream) – are managed on each side of the membrane. Due to the vapor pressure difference between the two air streams, the water vapor (moisture) is transferred from one into the other air stream as diffusion through the membrane layer.

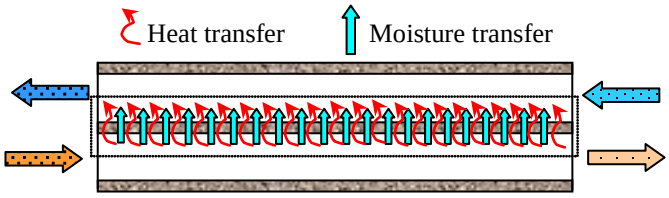

Fig. 1. Membrane-based heat exchanger or membrane-based air dehumidification unit with fresh air and exhaust air streams

EXPERIMENTAL SET-UP AND DATALOGGING

A membrane dehumidification unit (Zehnder ComfoAir 350) was installed in the laboratory of the Solar Energy Research Institute of Singapore (SERIS) as shown in Fig. 2. The ambient and exhaust air from a conditioned room is delivered by controllable fans. Temperature sensors (Omega Engineering INC, measurement range of -50 to 100˚C), relative humidity sensors (MICHELL PC 52, with accuracy of ±2% within 10 – 90% at 23 ˚C humidity), and air flow meters (Endress+Hausers, Prowirl 72F50) were installed at the inlets of the fresh air and exhaust air ducts.

Fig. 2. Test rig of the membrane-based air dehumidification unit

As illustrated in Fig. 3, a user-friendly and data logging system is established integrating National Instruments (NI) hardware CompactRIO and software LabVIEW.

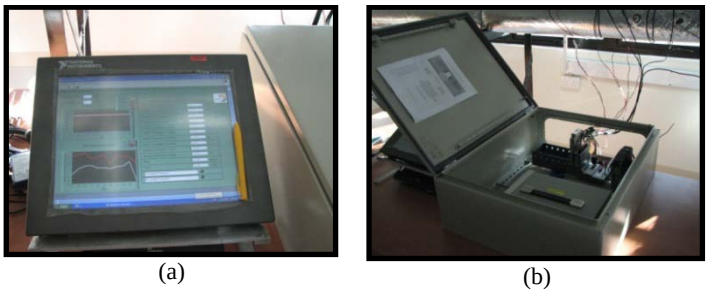

(a) (b)

(c)

Fig. 3. The LabVIEW data logging system of the membrane dehumidification unit: (a) Industrial Touch Panel Computer (Model TPC-2012) showing data logging system interface; (b) NI real-time controller CompactRIO (Model cRIO-9074) which allows the measurement data to be transferred to the TPC computer; (c) LabVIEW graphical programming interface for real-time data logging and monitoring.

NUMERICAL MODELING

The membrane dehumidification system is modeled using the finite element analysis software (COMSOL) for analyzing the moisture transfer process. As in Fig. 4, the simplified problem domain of the membrane heat exchanger is divided in three sub-domains $\Omega_i, i = 1,2,3$ – supply air channel Ω_1, exhaust air channel Ω_3, and the membrane layer Ω_2. Considering the symmetry of the channels allows modeling a half volume of air channels between two consecutive layers of membrane. The moisture permeation and heat transfer takes place between the supply air and exhaust air through the membrane. In this model, it is noted that the configuration of membrane heat exchanger is assumed as the configuration of the counter-flow plate heat exchanger (see Fig. 4).

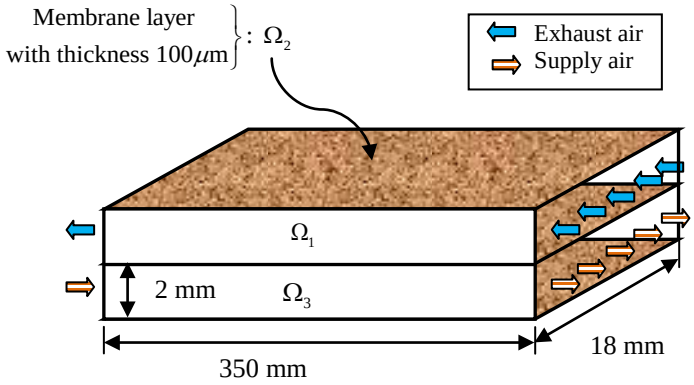

Fig. 4. Three-dimensional cross-flow plate heat exchanger with membrane barrier between the two air streams. This is an air-to-air heat exchanger using a membrane barrier instead of using a metal plate. It will recuperate latent heat from one air stream to another through the membrane.

The moisture transport process in the supply and exhaust air streams is governed by the convection and diffusion equation:

$$\nabla \cdot \left(-D_i \nabla c_i\right) = -\mathbf{u}_i \nabla c_i, \quad i = s, e \tag{1}$$

where c_i, D_i, and $\mathbf{u}_i$ are moisture concentration, diffusion coefficient and air velocity vector of "i" air stream, "s" refers to the supply air and "e" represents the exhaust air.

During the moisture permeation, the moisture from the supply air is firstly adsorbed into the surface of the membrane by

$$\left(-D_m \nabla c_m\right).\mathbf{n} = k_s \left(c_s - c_m\right). \tag{2}$$

The moisture is then transferred through the membrane core governed by the diffusion equation

$$\nabla \cdot \left(-D_m \nabla c_m\right) = 0. \tag{3}$$

Finally the moisture is released into the exhaust air stream from the membrane surface by

$$\left(-D_m \nabla c_m\right).\mathbf{n} = k_s \left(c_e - c_m\right) \tag{4}$$

where D_m is moisture diffusivity inside the membrane, $\mathbf{n}$ is unit normal vector, c_e, c_s and c_m are moisture concentration of exhaust air, supply air and inside the membrane, respectively. The term k_s is the convective mass transfer coefficient [15] :

$$k_s = \frac{Sh \times D_i}{L},\ i = s, e. \quad (5)$$

Sh is Sherwood number, and is evaluated by

$$Sh = 0.664 \times \sqrt{\mathrm{Re}} \times \sqrt[3]{Sc}, \quad (6)$$

where Re is Reynolds number

$$\mathrm{Re} = \left(\rho_i V_i L\right) / \mu_i, \quad (7)$$

and Sc is Schmidt number, respectively

$$Sc = \mu_i / \left(\rho_i D_i\right),\ i = s, e. \quad (8)$$

In Eqs. (5) to (8), ρ_i denotes the density [16] in kg/m^3, V_i represents the air velocity in m/s, μ_i is the dynamic viscosity of the air in $kg/(m.s)$ and L is the characteristic length in meter of the air channel, respectively.

As boundary conditions, moisture concentration of ambient air and that of conditioned air are imposed at the inlets of supply and exhaust air stream. The convective flux boundary condition, i.e., $\mathbf{n}.\left(-D_i \nabla c_i\right) = 0$ is dominated at the outlet of supply and exhaust air streams as mass flux due to the diffusion is negligibly small.

NUMERICAL AND EXPERIMENTAL RESULTS

Under Singapore climate, experiments were carried out in SERIS's laboratory. The same air volume flow rate for both supply and exhaust air were sent into the membrane unit. The supply air was taken from the ambient with the moisture content of 12 - 16 g/kg and the exhaust air was taken from a conditioned room where the humidity ratio was in the range of 8 - 11 g/kg. To arrive at the steady state condition of the air streams, the moisture content of the air streams and the air volume flow rate were adjusted every 30 minutes. The experimental data was recorded every 10 seconds. Finally, these recorded data were averaged and analyzed for the performance of the membrane dehumidification unit.

Numerical analyses have also been performed. The three dimensional nonlinear equations of the membrane unit are solved by the finite element method. The physical domain is descretized carefully as the aspect ratio of the membrane thickness and the length (and/or width) is very big. Membrane properties (that is mass diffusivity of water vapor inside the membrane, D_m in this case) needs to be imposed into the numerical model. However, it is very difficult to obtain the material properties of membrane material in practice. To identify D_m, simulation were carried out with parameters of supply and exhaust air used in the numerical simulation are given in Table 1.

Table 1. Supply and exhaust air properties for the numerical model

Description (Unit)	Supply Air	Exhaust Air
Temperature (˚C)	28	20
Dynamic viscosity ($kg.m^{-1}.s^{-1}$)	1.72×10^{-5}	1.69×10^{-5}
Air volume flow rate (m^3/h)	57	57
Humidity ratio (g/kg)	12.59	8.06

The humidity ratios of supply and exhaust air streams are converted to the moisture concentration to impose in the numerical model:

$$c_i = \frac{\omega_i \times \rho_i}{M_v} \quad (9)$$

where $\omega_i\left(kg/kg\right)$ is humidity ratio, $M_v\left(kg/kmol\right)$ is molecular weight of water vapour [16], and ρ_i is the densities. The densities of supply and exhaust air are calculated by

$$\rho_i = \frac{P}{R_{da} T_i}, \text{ and} \quad (10)$$

and diffusivities of supply air and exhaust air are evaluated by the following empirical equation [16]:

$$D_i = \frac{0.926}{P}\left(\frac{T_i^{2.5}}{T_i + 245}\right) \quad (11)$$

where T_i are temperatures (Kelvin) of "i" air stream, R_{da} is universal gas constant of dry air [16] in J/(kg.K), and P is air pressure in Pa.

The COMSOL simulation model was simulated for different mass diffusion coefficients at the air flow rate of 57 m^3/h. The error between the experimental data and numerical results are calculated at the outlets of supply and exhaust air streams:

$$\varepsilon_{\text{supply}} = \frac{\left(\omega_{s,out}\right)_{\text{simulation}} - \left(\omega_{s,out}\right)_{\text{experiment}}}{\left(\omega_{s,out}\right)_{\text{experiment}}} \quad (12)$$

and

$$\varepsilon_{\text{exhaust}} = \frac{\left(\omega_{e,out}\right)_{\text{simulation}} - \left(\omega_{e,out}\right)_{\text{experiment}}}{\left(\omega_{e,out}\right)_{\text{experiment}}} \qquad (13)$$

where the subscripts "*s*" represents the supply air, "*e*" represents the exhaust air, "*out*" denotes the outlet, "*in*" denotes for inlet (e.g., $\omega_{s,in}$ refers to the humidity ratio of supply air inlet condition), $\omega_{s,out}$ is the humidity ratio of supply air outlet, and $\omega_{e,out}$ is that of exhaust air outlet. In above equations, numerators are the humidity ratio difference between simulation and experiment results, and denominators represent the experimental data.

As in Fig. 5, the actual value of mass diffusion coefficient D_m is chosen as $3.5\times10^{-7}\ m^2/s$ at which the $\varepsilon_{\text{supply}}$ and $\varepsilon_{\text{exhaust}}$ are in balance and less than 5%.

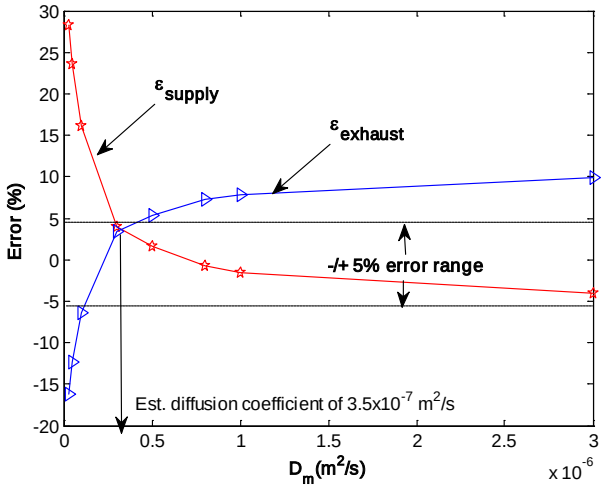

Fig. 5. Mass diffusion coefficient versus moisture removal at air volume flow rate of 57 m^3/h.

The COMSOL simulation result (see Fig.6) shows the nature of moisture transfer mechanism inside the membrane unit at 57 m^3/hr and $D_m = 3.5\times10^{-7}\ m^2/s$. It demonstrates that the moisture concentration of the supply air decreases along the air channel while the moisture concentration of the exhaust air increases due to moisture transfer through the membrane.

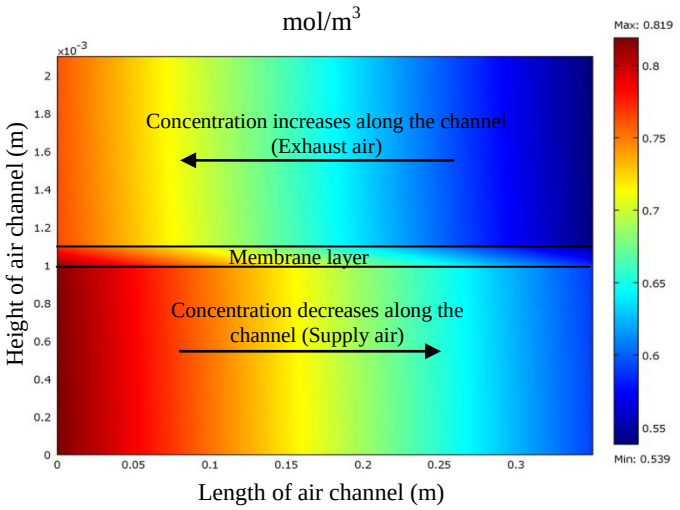

Fig. 6. Moisture concentration in the supply air, membrane and exhaust air stream at the air volume flow rate of 57 m^3/h.

Experimental data and numerical results for different air flow rates and different moisture concentrations of air streams were compared.

Fig. 7 and Fig. 8 plot the humidity ratio (in grams of water vapour per kilograms of dry air) of experimental and simulation results at the air volume flow rates of 57, 71 and 113 m^3/hr for which simulation results match well with the experimental data.

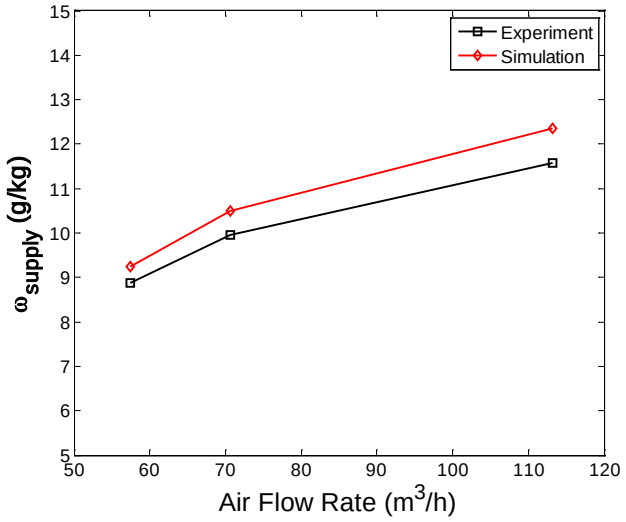

Fig. 7. Air volume flow rate (m^3/hr) versus humidity ratio at the outlet of supply air stream

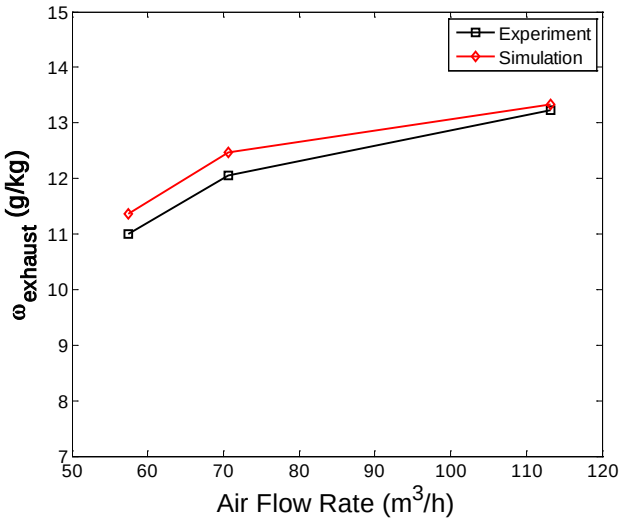

Fig. 8. Air volume flow rate (m^3/hr) versus humidity ratio at the outlet of exhaust air stream

Table 2 shows recorded experimental and simulation data including the humidity ratios of supply air inlet ($\omega_{s,in}$), supply air outlet ($\omega_{s,out}$), exhaust air inlet ($\omega_{e,in}$), exhaust air outlet ($\omega_{e,out}$), and error percentage. It is found that $\omega_{s,out}$ agrees well with the experimental data within uncertainty of within ±7% for different air flow rates, and $\omega_{e,out}$ agrees with the experiments within ±4% uncertainty. Uncertainty most probably comes from (i) the accuracy of the sensor and (ii) truncation or rounding error during numerical simulation.

Table 2. Humidity ratios (g/kg) of supply air and exhaust air

m^3/h		Absolute humidity (g/kg)			
		Supply air inlet $(\omega_{s,in})$	Supply air outlet $(\omega_{s,out})$	Exhaust air inlet $(\omega_{e,in})$	Exhaust air outlet $(\omega_{e,out})$
57	Exp	12.59	8.88	8.06	10.99
	Sim	12.59	9.24	8.06	11.37
	Error	-	-4.05%	-	-3.46%
71	Exp	14.08	9.97	8.97	12.06
	Sim	14.08	10.50	8.97	12.48
	Error		-5.32%		-3.48%
113	Exp	15.19	11.58	10.53	13.23
	Sim	15.19	12.36	10.53	13.32
	Error	-	-6.74%	-	-0.68%

Using the promising simulation results, the latent effectiveness

$$\eta_{Lat} = \frac{\left(\omega_{s,in} - \omega_{s,out}\right)}{\left(\omega_{s,in} - \omega_{e,in}\right)} \qquad (14)$$

is defined, evaluated and plotted in Fig. 9. It is observed that maximum latent effectiveness can be 0.74 and the figure describes the behaviour of latent effectiveness with respect to air volume flow rate. The latent effectiveness decreases with increasing air flow rates.

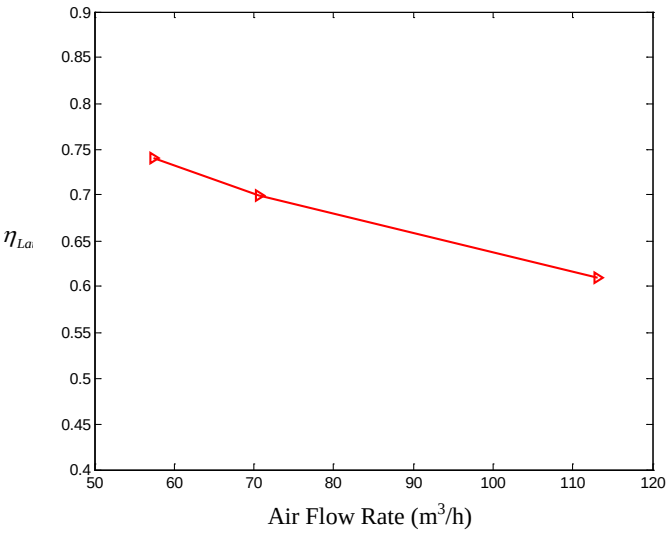

Fig. 9. Latent effectiveness versus supply air volume flow rate (m^3/h).

To facilitate the analyses, the latent heat handled by the membrane dehumidification unit is calculated using Eq. (15):

$$Q = \Delta\omega \times \dot{m} \times h \qquad (15)$$

where $\Delta\omega$ is the amount of moisture removed from the supply air after passing the membrane unit, $\dot{m}$ is air flow rate in kg/s, and h is the specific enthalpy for saturated water vapor [16] at the temperature of the air:

$$h = h_{fg} + \alpha t \qquad (16)$$

where $h_{fg} = 2501\ kJ/kg$ is latent heat of vaporization at 0 ˚C, $\alpha = 1.805\ kJ/(kg.C)$ is specific heat of water vapor, and t is the air temperature in degree Celsius. Table 3 shows the properties and the specific enthalpy of air for different experiments.

Table 3. The air flow rate, air temperature and specific enthalpy of water vapor

m^3/hr	$\dot{m}(kg/s)$	T (°C)	h (kJ/kg)
57	1.86×10^{-2}	28	2552
71	2.32×10^{-2}	27	2550
113	3.68×10^{-2}	28	2551

Table 4 (second column) shows the latent load removed by the membrane dehumidification unit. For the comparison between the MEMbrane dehumidifier (MEM), Desiccant Dehumidifier (DD) and conventional dehumidification by CHilled water (CH), energy demand of each system for handling latent load is calculated based on the assumptions of (i) using a desiccant dehumidifier with a reasonable thermal COP (cooling capacity in kW by the required heat energy input in kW for regeneration) of 0.5 and (ii) using a high efficiency chiller with the COP (cooling capacity in kW by its electric energy input in kW) of 4. From the calculation (see Table 4), the desiccant dehumidifier requires the heat energy and the conventional dehumidification requires electric energy to handle latent loads while the membrane technology does not consume electric and heat energy. However, it is noted that the membrane dehumidification needs the return air from the conditioned room for the moisture transfer.

Table 4. Latent load handling and energy demand comparison of the membrane unit, a desiccant dehumidifier and an high efficient chiller

m^3/h	Q (W)	Tech-nology	COP_{th} ‡	COP§§	Input electri-city (W)	Input heat (W)
57	177	MEM*	-	-	-	-
		DD†	0.5	-	-	353
		CH§	-	4	44	-
71	243	MEM	-	-	-	-
		DD	0.5	-	-	486
		CH	-	4	61	-
113	389	MEM	-	-	-	-
		DD	0.5	-	-	778
		CH	-	4	97	-

*MEM = membrane unit

†DD = Desiccant dehumidifier

§CH = Chiller

‡COP_{th}= $\dfrac{\text{Cooling capacity in kW}}{\text{Required heat energy in kW for regeneration}}$

§§$COP = \dfrac{\text{Cooling capacity in kW}}{\text{Electric energy input in kW}}$

CONCLUSIONS

The membrane dehumidification was investigated through the numerical analyses and experiments. The moisture from the ambient air can transfer through the membrane because of the moisture concentration gradient between air streams. Based on our analyses, we found that:

i. Within the air flow rate of 57 to 114 m^3/h, the average moisture transfer rate is approximately in the range of 3 to 5 g/kg.
ii. The membrane based air dehumidification unit does not consume both thermal and electric energy because the dehumidification takes place due to the gradient in humidity between air streams.
iii. no chemical reaction occurs during dehumidification

Therefore, under the assumption that sufficient suitable exhaust air is available, the membrane system can be employed as an efficient air dehumidification for air conditioning applications in particular in tropics where latent load constitutes a large portion of total cooling load handled by an air conditioning system.

ACKNOWLEDGMENTS

The authors would like to thank to the Clean Energy Research Program Office (CEPO), Singapore for the financial support during the course of this work. Finally, the authors would like to thank Professor LUTHER Joachim (CEO, SERIS) for his suggestions and discussions during the course of this work.

REFERENCES

1. Ge, T.S., Li, Y., Wang, R.Z., Dai, Y.J., 2008, A review of the mathematical models for predicting rotary desiccant wheel. Renewable and Sustainable Energy Review. 12, pp.1485-1528.
2. Kim, D.S., Infant Ferreira., C.A., 2009, Air-cooled LiBr-water absorption chillers for solar air-conditioning in extremely hot weathers. Energy Conversion and Management, 50, pp.1018-1025.
3. Panaras, G., Mathioulakis, E., Belessiotis, V., Kyriakis, N., 2009, Theoretical and experimental investigation of the performance of a desiccant air-conditioning system. Renewable Energy, 1-8.
4. Kanoglu, M., Carpinlioglu, M.O, Yildirim, M., 2004, Energy and exergy analyses of an experimental open-cycle desiccant cooling system., Applied Thermal Engineering, 24, pp.919-932.
5. Zhai, X.Q., Wang, R.Z., Wu, J.Y., Dai, Y.J., Ma., Q., 2008, Design and performance of a solar-powered air-conditioning system in a green building. Applied Energy., 85, pp.297-311.
6. Hao, X., Zhang, G., Chen, Y., Zou, S., 2007, Demetrios. J. Moschandreas, A combined system of chilled ceiling,

displacement ventilation and desiccant dehumidification, Building and Environment., 42, pp.3298–3308.
7. Tomaszewska, M., Gryta, M., Morawski, A.W., 2000, Mass transfer of HCL and H2O across the hudrophobic membrane during membrane distillation. Journal of Membrane Science., 166, pp.149-157.
8. Niu, J.L., Zhang., L.Z., 2001, Membrane-based enthalpy exchanger: material considerations and clarification of moisture resistance. Journal of Membrane Science., 189, pp.179-191.
9. Zhang, L.Z., Jiang., Y., 1999, Heat and mass transfer in a membrane-based energy recovery ventilator. Journal of Membrane Science., 163, pp.19-38.
10. Zhang., L.Z., 2009, Heat and mass transfer in plate-fin enthalpy exchangers with different plate and fin materials. International Journal of Heat and Mass Transfer., 52, pp.2704-2713.
11. Zhang, L.Z., Niu, J.L., 2009, Effective correlations for heat and moisture transfer processes in an enthalpy exchanger with membrane cores. Journal of Heat Transfer., 124, pp.922-929.
12. Scovazzo, P., Hoehn, A., Todd, P., 2000, Membrane porosity and hydrophilic membrane-based dehumidification performance. Journal of Membrane Science., 167, pp.217-225.
13. Liu, S., Riggat, S., Zhao, X., Yuan., Y., 2009, Impact of adsorbent finishing and absorbent filming on energy exchange efficiency of an air-to-air cellulose fibre heat and mass exchanger., Building and Environment., 44, pp.1803-1809.
14. Ito, A., 2000, Dehumidification of air by a hygroscopic liquid membrane support on surface of a hydrophobic microporous membrane. Journal of Membrane Science., 175, pp.35-42.
15. Tosun, I., 2001, Modelling in transport phenomena: A conceptual approach. Elsevier, Amsterdam, Netherlands.
16. ASHRAE Handbook (2010).